Bilder: Tabellen:

Mullitization Behaviour during Thermal Treatment of Three Kaolinitic Clays from Cameroon: Densification, Sintering Kinetics and Microstructure

C. Leonelli, E. Kamseu, U.C. Melo, A. Corradi, G. C Pellacani

Mr Elie Kamseu graduated from the University of Yaounde I, Cameroon, with a BSc in Chemistry (1998), followed by two MSc degrees in Inorganic Chemistry (2000 and 2002). Since 2003 he has been working towards a PhD thesis (now on the final stage) in the field of ceramic and glass materials in collaboration with the department of Materials and Environmental Engineering of the University of Modena and Reggio Emilia (Italy). His special research interest focuses on the mechanical properties of ceramics and glass-ceramic materials. He has authored several articles and research reports in the field of valorisation of mineral resources, glass-ceramics and quality control of materials. His current position is researcher at the Local Materials Promotion Authority (MIPROMALO) in Cameroon.

Abstract

Three kaolinitic clays from Cameroon were studied for their mullitization behaviour. The three clayey materials were from Ntamuka (TAN), Mayouom (MAY) and Wabane (WAB), all situated in the hills of western Cameroon. X-ray diffraction and thermal, dilatometric and SEM-EDS analyses were used to follow up the phase evolution, sintering kinetics and microstructure of the three materials as a function of temperature (1000–1500 °C). Fine powders of each sample were pressed and treated in the above temperature range with the goal to correlate the phase evolution with densification parameters (shrinkage, porosity, density and mechanical strength). The nucleation of mullite and the increase of peak intensities were directly correlated to continuous densification and reduction of open porosity as observed under the SEM. The mullitization peak temperatures at 5 °C/min were 973 °C, 979.1 °C, and 983.6 °C respectively for TAN, MAY and WAB and – in the same order but at 20 °C/min - 992.1 °C, 997.4 °C and 1001.2 °C. The mullitization phenomenon, which includes a first step of nucleation and a second of crystal growth, shows an activation energy that varies depending on the nature of sample investigated: the values ranged from 650 to 730 kJ/mol. The microstructure of the sintered products consisted on the elongated secondary mullite (types II and III) interlocking with primary (type I) mullite in a compact matrix with relative amount of liquid film for MAY and WAB. The morphology of mullite grains in TAN was more different being larger cuboid grains aggregated with cristobalite to form a compact microstructure. The formation of TiO_2 crystals and then Ti-Al (tialite: Al_2TiO_5) crystals influenced the microstructure of MAY and WAB.

Keywords: mullitization, densification, microstructure, activation energy, grain morphology

1 Introduction

Mullite is the most stable compound of the system Al_2O_3–SiO_2 under ordinary conditions. It exhibits attractive properties for refractory ceramics: high refractoriness, low thermal conductivity, and low thermal expansion properties at high temperatures. The formation of mullite during the sintering of porcelain is very important since mullite is the most significant crystal as constituent of this highly resistant ceramic product. In this case, kaolin and kaolinitic clays are used because they are the cheapest source of Al_2O_3-SiO_2. Clays with $\leq$60 % Al_2O_3 convert to mullite during heat treatment. The amount of mullite produced is directly related to the Al_2O_3 content and the calcination temperature. Kaolin with high purity and good crystallinity will develop mullite crystals starting from 950 °C, while disordered kaolin will promotes mullite at relatively high temperatures (1200 °C). The impurities included in these materials will influence the overall amount of mullite produced [1–3]. Owing to the impurities, mainly alkalis and iron, local melting may occur at low temperatures. The liquid phase is generated by low-temperature melting of impurities (various sheets of silicates, ilmenite, and iron oxides, i.e. hematite and goethite) in the presence of quartz. These elements, usually metallic ions (Fe^{3+}, Ti^{4+}, …) generally act as catalysts for thermo-chemical reactions. The formation of a liquid phase promotes ion diffusion and allows mullitization to occur through a dissolution-precipitation mechanism. Fe^{3+} and Ti^{4+} are well known as nucleating agents of crystallization in the presence of liquid phase [2–3]. Castelein et al. [4] described the influence of the grade of kaolin in terms of crystallinity and purity, and the heating rate on phase transformation during the formation of mullite. They suggested that such phase transformation included the presence of an intermediate γ-alumina derived spinel. As a consequence the amount and the morphology of mullite crystals depend on possible interactions among all these minerals. Concerning the morphological aspect of the studies of mullite crystals a relationship to the initial stoichiometry of the materials should be considered. The general formula of mullite is $Al_2[Al_{2+2x}Si_{2-2x}]O_{10-x}$, where x denotes the number of vacancies formed by the ex-solution of octahedral O atoms. The $Al_{4.5}Si_{1.5}O_{9.75}$ generally assimilated to $3Al_2O_3{\cdot}2SiO_2$ designated as 3/2-mullite with x = 0.25 is generally synthesized at relatively low temperatures (1000 °C) from aluminosilicates while the $Al_{4.8}Si_{1.2}O_{9.2}$ generally assimilated to $2Al_2O_3{\cdot}SiO_2$ (2/1) mullite has more alumina with x = 0.4 and results from thermal activation of 3/2-type at high temperature (1400 °C). The high aluminous mullites change their composition toward stoichiometric 3/2-

mullite [6–7]. Mullite needles initiate nucleation with low alumina content, the concentration of alumina increasing with temperature; at very high temperatures mullite promotes the formation of corundum [8–9], a reaction that explains the progressive decrease of silica in the mullite structure with decreasing ((??)) temperature. Moreover, the orientation of mullite from 3 : 2 to 2 : 1 depends essentially on the temperature, composition of the starting materials, and thermo-chemical reaction parameters. The present paper investigates the mullitization behaviour during sintering of three kaolinitic clays mined in Cameroon. In recent years geologists and researchers demonstrated the potential of Cameroon in term of clay resources [10]. Three samples of kaolinitic clays geologically investigated [11–12] were chosen for studies of their behaviour in mullitization during thermal treatment. Kinetic theories [2–6] based on the DTA and dilatometric analysis supposed that the maximum crystallization rate is at the DSC peak temperature. The Johnson-Mehl-Avrami [2–6] equation is the most important theoretical basis. It describes the evolution with time t of the volume fraction crystallized x with nucleation frequency I_v and the crystal growth rate U. When I_v and U are supposed to be independent of time, then the integral form is:

((please check symbols in text and formula))

$$x = 1 - \exp\left(-g' I_v U^{n-1} t^n\right) \quad (1)$$

where g' is a geometrical factor related to the growing phase and n is an integer which depends on the crystallization mechanism. Regarding the microstructure, fired kaolin above 1200 °C shows cuboid mullite grains that were found to be primary mullite [7–9]. Secondary mullite should be present, with morphology and size influenced by the chemical composition of the parent clay. At higher temperatures (≥1300 °C), iron favours the growth of large mullite crystals embedded in the silico-aluminate matrix, up to about 60 % of the total volume [17]. The shape of nuclei is constrained as a function of the total surface energy and the coherence between the matrix phase and the daughter nuclei. Authors [16] described the microstructure of mullite/mullite nano-composite powder as composed of nano-sized 3:2 inclusions within 2:1 matrix. It was reported that potassium ions promote pure phase mullite formation with shaped and acicular crystals, while sodium and calcium ions promote cristobalite and needle shaped mullite crystals during the thermal treatment of kaolin [18].

The amount of liquid formed at sintering temperatures, and the time after which ((??please check, duration at which is not right)) crystallization takes place determine the chemical composition and the aspect ratio of secondary mullite. The microstructure of the fired specimens with different Al_2O_3/SiO_2 ratios and amounts of impurities were correlated to densification and mechanical properties. Microstructural investigations were used to evaluate the crystallization behaviour, the quality of mullite formed, and the influence of various impurities contained in each of the kaolinitic clays under study.

2 Experimental procedure

2.1 Starting materials

The three kaolinitic clays used in this study were Wabane clay (WBN), Mayouom clay (MAY) and Ntamuka clay (TAN). All the three deposits are situated in western Cameroon, in a region of high hills. The chemical composition is listed in Table 1. TAN is a sand clay with 50 % kaolinite and 40 % quartz together with minor additional phases. WAB and MAY are two clays with 75–80 % kaolinite and less than 10 % quartz. Apart from these two minerals, MAY contains illite, anatase, hematite and ilmenite, while WAB has ilmenite and anatase. Geologists distinguish sandy-MAY and low-sand MAY [12]. In this study low-sand-MAY was used. The three samples as collected in the field were stored for months, dry ground and ball-milled to homogeneous fine powders (<80 µm).

2.2 Green compact formation and sintering

Fine powders of the three kaolinitic clays were wet pressed (10 mass-% of water) to form compacted discs of 40 mm × 5 mm under uni-axial 29 bar. ((wet pressed under 2.9 MPa ...??)) These specimens were dried at room temperature for 72 h and in a dryer (110 °C) for 24 h. The specimens were then fired in an electric furnace from 1000–1500°C with intervals of 100 °C. The firing rate was 10 °C/min, with 4 h soaking time at 1000, 1100 and 1200 °C. At high temperatures (1300, 1400 and 1500 °C), 2 h soaking time was chosen. All the samples were left to cool in the furnace.

2.3 DTA, DSC and dilatometry ((please check: DTA was missing in the headline; please also check the green part of this paragraph for correctness/completeness))

Differential thermal analysis (DTA) was performed on fine ground powder of the three samples with heating rates of 5, 10, 15 and 20 °C/min up to 1300 °C. Differential scanning calorimetry (DSC), a similar analysis, was performed under identical conditions for dilatometry. The use of the Kinsinger theory for kaolin-mullite sintering in the context of this work is based on the consideration that mullite is the essential crystallization product and responsible for the maximum peak in the case of DSC and non variation of linear shrinkage near the temperature of mullitization for the optical dilatometry analysis. In non-isothermal conditions at a constant heating rate v and after integration of Equation (1) becomes: ((sentence is not clear))

$$\ln\left(\frac{v}{T_x^2}\right) = \left(\frac{-E_{\sin}}{RT_x}\right) \quad (2)$$

where T_x is the temperature at which the sintering process attains a constant shrinkage value X. A plot of $\ln\left(v/T_x^2\right)$ versus $1/T_x$ in the case of DSC and dilatometry curves at different firing rates should give a straight line whose slope is $E_{\sin}/R$. The temperatures of the mullitization peak for each heating rate were used for DSC while those of constant shrinkage near the mullitization peak were used for dilatometry.

2.4 Densification of fired specimens

The densification behaviour of the three kaolinitic clays was evaluated in terms of bulk density and bending strength. The bending strength was determined using the biaxial flexural strength test in accordance with ASTM F394-78 [14]. The fired specimens were centred and supported on three steel balls (2.67 mm diameter) positioned at 120° offset around the circumference (9.5 mm diameter) and loaded in a material testing machine (MTS, type 810, USA) with a crosshead speed of 3 mm/min.

2.5 Microstructure

Pieces of samples of three kaolinitic clays fired in the range of temperatures 1000-1500 °C were used for the microstructural investigations. The samples were coated with resin and polished using 3 and 1 μm alumina pastes after grinding with silicon carbide powders and water. The polished surfaces were etched for 10 min in 4 % HF-HNO_3 solution and then gold coated to prepare them for examination under the scanning electron microscope (PSEM500, PHILIPS XL30). Microanalysis was performed using EDS (X_EDS INCA, Oxford Inst.). For determination of the chemical composition, a minimum of 20 spots were included in each analysis. The fired specimens were finely ground and the powders obtained were subjected to X-ray analysis. The XRD was performed using a diffractometer with goniometer PW3050/60 (theta/theta), Ni filtered Cu Kα radiation (40 kV, 40 mA).

In order to understand the properties of these materials the powder diffraction technique "Rietveld Method" using material in the form of very ?? ((fine??)) powder (small crystallites) was used. The drawback of the conventional powder diffraction method is that the major overlap of the data it provides prevents a proper determination of the structure. The height, width and position of the diffraction peaks are used to determine many aspects of the material's structure. The "Rietveld Method" creates an effective separation of these overlapping data, thereby allowing an accurate determination of the structure. The Rietveld Method was therefore also used for quantitative phase evaluation.

3 Results

3.1 Phase evolution

All the three samples of kaolinitic clays presented an amorphous structure up to 1100 °C with poor densification behaviour. Phases such as γ-Al_2O_3, SiO_2 and spinels ($SiAl_2O_5$) were detected, along with minor nucleids of mullite. For T ≥1100 °C:

$SiAl_2O_4$ (spinel) + SiO_2 (amorphous) →$3(3Al_2O_3{\cdot}2SiO_2)$ (mullite) + $4SiO_2$ (amorphous) could be considered as principal thermo-chemical reaction; or

Al_2O_3 (γ-alumina) + $2SiO_2$ (amorphous) →$3(3Al_2O_3{\cdot}2SiO_2)$ (mullite) + $4SiO_2$ (amorphous) ((this sentence is not complete)).

For T ≥1200 °C: amorphous silica gradually transforms into cristobalite, while for T ≥1500 °C, cristobalite transforms again into amorphous silica. It was observed that mullite formation was lower in TAN than in WAB and MAY (Fig. 1), obviously due to the low alumina content of the sample (24.88 %). Furthermore, the presence in the sample of a considerable amount of silica presumably justifies the formation of cristobalite at the expense of mullite. In fact, when Al_2O_3 is present in the matrix, it should react easily with amorphous silica to form mullite. But when Al_2O_3 is low in the matrix, and in some thermo-chemical conditions (T ≥1200 °C), the amorphous silica crystallizes to cristobalite as indicated in the above equations. At high temperatures, mullite peak intensities increase while those of quartz decrease: we can here suggest the hypothesis of mullite grain growth (Fig. 2) by the phenomena of silica enrichment with the transformation of 3/2 mullite to 2/1 mullite as confirmed by literature [6–8]. The basic difference between the three samples is the Al/Si ratio that correlated with the presence of impurities (Fe_2O_3, Na_2O, K_2O and TiO_2), which partially explains the results described above. In all the samples, thermal treatment influenced the mullite content in the matrix as described elsewhere [15].

3.2 Correlation crystallization-densification

It is important to note that the study of the crystallization behaviour is related to the density, surface area, shrinkage and some other sintering parameters that correlate favourably with the sintered properties. In the temperature range of 1000–1100 °C, as revealed by XRD patterns, the fired specimens are characterized by their amorphous nature due to the decomposition of kaolin. Metakaolin, spinel, and mullite needles are dispersed in the microstructure with high specific surface area. Metakaolin is transformed to mullite grains while, with temperature development ((increasing temperatures??)), mullite needles progressively form aggregates with a decrease in specific surface area [6–9]. The sintering behaviour here can be described by surface transport which involves neck growth without densification due to the mass flow originating and terminating at the particle surface, and to surface diffusion. Between 1100 °C and 1200 °C, the density and mechanical properties (Figs. 3 a and 3 b) increase rapidly. At this stage of sintering, density correlates to volume and grain boundary diffusion, as well as plastic and viscous flow with initial liquid film formation. The associated bulk transport will create a change in inter-particle spacing as neck growth takes place. The existing crystals or nucleids will then impose the crystallization rate and, as a result, the change in shrinkage and densification behaviour (Figures density and mechanical??).

3.3 Sintering kinetics

DSC, non-contact dilatometry, SEM-EDS and densification behaviour were used to investigate the parameters that govern the kinetics during sintering. The mullitization DSC peak and dilatometry plateau varied as a function of the Al/Si ratio and was influenced by the sintering rate. The mullitization temperatures at 5 °C/min were 973 °C, 979.1 °C, and 983.6 °C respectively for TAN, MAY and WAB and – in the same order but at 20 °C/min – 992.1 °C, 997.4 °C and 1001.2 °C. Decreasing the sintering rate will be progressively sensitive ((critical??)) for the pore-grain boundary morphology. Li and Thomson analyzed kinetic mechanisms from ((in??)) different sol-gel precursors using dynamic X-ray diffraction and DSC and found a significant change in activation energy as a function of the Al/Si ratio. In the case of the kaolinitic clays under study, the activation energy was 657.00 ±99.54, 671.47 ±108.08 and 722.61 ±112.94 $kJ{\cdot}mol^{-1}$ respectively for TAN, MAY and WAB applying the non-isothermal DSC method. For dilatometry and using the same non-isothermal method, the activation energy was 686.76 ±117.31, 649.01 ±84.71 and 731.29±110.63 $kJ{\cdot}mol^{-1}$ respectively (Fig. 4). These results can be correlated to the Al_2O_3/SiO_2 ratios of the three kaolinitic clays. In fact, it seem that the higher the value of the Al_2O_3/SiO_2 ratio, the more

significant the activation energy. The Al_2O_3/SiO_2 ratios are 0.4, 0.71 and 0.81 respectively for TAN, MAY and WAB. Apart from the Al/Si ratio, different crystallization processes and experimental conditions can be used to explain the range of error and the difference in the activation energy level in mullite sintering (Fig. 4). The Fe^{3+} and Ti^{4+} ions are known [2–3] for their capacity to enhance the crystallization of mullite, but the low amount of these ions and the relatively low Al_2O_3 content (≈25 %) compared to the others (34 %) can explain the densification behaviour of TAN. The formation of liquid film provides the benefit of a surface tension acting to aid densification and pore elimination. The pores become fewer in number and diminish in size due to shrinkage. Above this temperature no significant crystallization did took place. This can be correlated to X-ray diffraction results (Fig. 1) with no significant variation in mullite peaks between 1300 and 1500 °C. MAY at 1400 °C presented the formation of a sufficiently extended liquid film capable of filling residual pores, resulting in maximum densification of this sample (Fig. 3a). Although the WAB and MAY samples both have similar SiO_2/Al_2O_3 ratios; the similarity of the mechanical strength values is limited at 1200 °C where WAB showed its maximum (60 MPa). The presence of fissures in the samples above 1300 °C can explain the decline in mechanical properties. WAB contains ≥4 % TiO_2 and 1 % of Fe_2O_3 which should play an important role in the mullitization phenomenon with direct correlation to densification. The absence of a sufficient amount of liquid (low Na_2O+K_2O content compared to MAY) contributes to the segregation of various crystals. The low fracture properties of tialite composites are due to extensive microcracking during cooling from the firing temperature [19]. The alumina titanite crystal (tialite) is isomorphous with pseudobrookite, crystallizing in the orthorhombic space group Cmcm and is characterized by pronounced anisotropy in the thermal expansion coefficient, resulting in a distinct hysteresis [18–19]. This pronounced anisotropy is the reason for severe microcracking during cooling which leads to the poor mechanical properties of sintered WAB compared to sintered MAY (Fig. 5). The microcracking phenomenon is closely related to the material's microstructure. Below a critical grain size, the elastic energy of the system is insufficient for microcrack formation during cooling and thus the mechanical properties are considerably enhanced. This is the case for the samples of MAY and WAB up to 1200 °C. The less pronounced decrease in mechanical properties of MAY compared to WAB at 1200 °C is probably attributable to the difference in Fe_2O_3 as well as (to a minor extent) MgO contents which are supposed to act as stabilizers [18–19]. The more pronounced presence of liquid film in MAY can be an additional effect of stabilization. TAN presented a microstructure influenced by a high proportion of silica crystals (both quartz and cristobalite) with rod-like or granular mullite grains in the interstice regions (Figs. 6–7). As shown in Fig. 2, the grain size of mullite increases with temperature. From 0.04 µm at 1100 °C as determined by the Rietveld method, the mullite nuclei grow progressively to 0.1 µm at 1300 °C and 0.5 µm or 0.6 µm at 1500 °C. These values are similar to those obtained by Chin-Yi et al. [3]. In their work on the evolution of mullite texture on firing tape-cast kaolin bodies, the mullite grains obtained had grain sizes less than 1 µm up to 1500 °C with intensive grain growth between 1400 and 1500 °C as in the case under study. On the matrix, individual larger grains can be observed with dimensions more than 1 or 2 µm, especially at 1400 and 1500 °C (Figs. 6–7). This type of mullite, characterized by its elongated shape, is generally present in areas of glass concentration being alkali-dependent ((what is alkali-dependent- glass concentration or grain growth of this mullite type?? please check/re-write.)) [4]. Auhors [8] has also demonstrated the influence of iron on the growth of mullite grains but the iron oxide content in our samples was too low for a comparison. However we could attribute the relative difference in growth behaviour and grain size between the three kaolinitic clays to the proportion of metallic oxides present in each composition.

4 Conclusion

The densification behaviour of three kaolinitic clays from Cameroon revealed refractoriness. The densification behaviour results in relatively porous materials apart from Mayouom clay where the significant alkali content results in the formation of liquid film capable of embedding crystalline phases and filling residual intergranular pores. The different densification behaviour and mechanical properties was due to the formation of additional phases, i.e. cristobalite for TAN, and Ti-Al compounds (i.e. tialite: Al_2TiO_5) for MAY and WAB, with varying effects on the final properties. The difference in the temperature at which mullite started to form, 1100 °C for MAY and WAB and 1200 °C for TAN, is an indication of the degree of crystallinity of the three clayey materials.

- The activation energy of mullite crystallization calculated by the non-isothermal method (Kissinger method) using both DSC and non-contact dilatometry was in the range of 650 and 731 $kJ \cdot mol^{-1}$, which was in agreement with literature and demonstrated that non-contact dilatometry is an adequate method for studying mullite crystallization.
- It was assumed that there is correlation between the sintering kinetics of mullitization and the densification parameters of the three kaolinitic clays studied.

Orthorhombic crystals of mullite were identified as the major phase developed during sintering of three kaolinitic clays from Cameroon in the space group pbam. Mullite grains showed an average alumina ratio of 2:1 but it was found that the microstructure of the fired product of the three kaolinitic clays can be described as interlocking of secondary (types II and III) elongated mullite with cuboid primary mullite (type I), with the alumina-silica ratio varying from 1:1 to 2-5:2, depending on the raw composition and impurities. MAY and WAB developed more elongated Al-rich mullite, especially in regions of glassy film concentration. Between 1200 and 1300 °C the formation of TiO_2 and $Al_2O_3.TiO_2$ crystals was responsible for the presence of fissures of cracks (fissures or cracks?? /

microcracks??)). In WAB, TiO_2 crystals decrease progressively with temperature development ((with lower / higher temperatures??)). Both these two Ti-rich crystals seem to be instable with temperature. ((not clear))

Acknowledgement

The authors of this article wish to express their gratitude to the University of Modena and Reggio Emilia for the support granted to Elie Kamseu (Research grant No 10679).

References

[1] Mackenzie, K.J.D., Meinhold, R.H., Brown, I.W.M., White, G.V.: The Formation of Mullite from Kaolinite under Various Reaction Atmospheres, J. Europ. Ceram. Soc. **16** (1996) 115–119

[2] Romero, M., Martin-M, J., Rincon, J.Ma.: Kinetic of mullite formation from a porcelain stoneware body for tiles production , J. Europ. Ceram. Soc. **26** (9) (2006) 1647–1652

[3] Traoré, K., Gridi-Bennadji, F., Blanchart, P.: Significance of kinetic theories on the recrystallization of kaolinite. Thermochimica Acta **451** (2006) 99–104

[4] Castelein, O., Soulestin, B., Bonnet, J.P., Blanchart, P.: The influence of heating rate on the thermal behaviour and mullite formation from a kaolin raw material, Ceramic Internat. **27** (2001) 517–522

[5] Chakravorty, A.K., Ghosh, D.K.: Kaolinte mullite reaction series: Development and significance of a binary alumino-silicate phase. J. Amer. Ceram. Soc. **74** (1991) 1401–1406

[6] Ribeiro, Tulyagavov, D.U., Ferreira J.M., Labrincha, J.A.: High temperature mullite dissolution in ceramics bodies derived from Al-rich sludge. J. Europ. Ceram. Soc. **25** (2005) 703–710

[7] Chen, Y.F., Wang, M.C., Hon, M.H.: Transformations kinetics for mullite in kaolin-Al_2O_3 ceramics. J. Mater. Res. **18** [6] (2003) 1355–1362

[8] Schumucker, M., Hildmann, B., Schneider, H.: Mechanism of 2/1- to 3/2-mullite transformation at 1650 °C. Amer. Min. **87** (2002) 1190–1193

[9] Lu, H.Y., Wang, W.L., Tuan, W.H., Lin, M.H.: Acicular Mullite crystals in vitrified Kaolin. J. Amer. Ceram. Soc. **87** [10] (2004) 1843–1847

[10] Kamseu, E.: Effets des fondants sur le comportement de quelques argiles du Cameroun entre 950 °C et 1050 °C Mémoire de Maîtrise. Dept. Chim. Ing. Université de Yaounde **1** (2000) 63

[11] Chinje Melo, U.F., Kamseu, E., Djangang, C.: Effect of fluxes on the fired properties between 950–1050 °C of some Cameroonian clays. Tiles & Bricks Internat. **19** [5] (2003) 384–390

[12] Njoya, A., NKoumbou C., Grosbois, C., Njopwouo, D., Njoya, D., Courtin-Nomade, A., Avon, J., Martin, F.: Genesis of Mayouom Kaolin deposit (Western Cameroon), Applied Clay Science **32** (2006) 125–140

[13] ASTM C20-00: Stantard test methods for apparent porosity, water absorption, apparent specific gravity, and bulk density of burned refractory bricks and shapes by boiling water

[14] ASTM F394-78: Standard test method for biaxial flexure strength (Modulus of rupture) of ceramics substrates

[15] Kamseu, E., Braccini, S., Corradi, A., Leonelli, C.: Mullitization behavior during thermal treatment of three kaolinitic clays from Cameroon. Part 2: Microstructure. Article in preparation.

[16] Dabbs, Daniel M., Yao, Nan, Aksay Ilhan A.: Nanocomposite mullite/mullite powders by spray pyrolysis. Journal of Nanoparticle Research 1: (1999) 127–130

[17] Djemai, A., Balan, E., Morin, G., Heermandez, G., Labbe, J.C., Mulller, J.P.: Behaviour of paramagnetic iron during the thermal transformations of kaolinite, J. Amer. Ceram. Soc. **84** (5) (2001) 1017–1024

[18] Yamuna, A., Devanarayanan, S., Lalithambika, M.: Phase-pure Mullite from caolinite, J. Amer. Ceram. Soc. **85** (2002) [6] 1409–1413

[19] Tsetsekou, A.: A comparison study of tialite ceramics doped with various oxide materials and tialite-mullite composites: microstructural, thermal and mechanical properties. J. of Europ. Ceram. Soc. **25** (2005) 335–348

Received: 13.02.2008

Captions

Fig. 1 Variation of the intensity of mullite peaks of fired samples as function of temperature
Author please add these corrections to your Fig. 1:
Horizontal axis: Temperature / °C
Vertical axis: Mullite peaks / mm

Fig. 2 Grains growth of mullite as function of temperature
Author please add these corrections to your Fig. 2:
Horizontal axis: Temperature / °C
Vertical axis: Grain size / µm
Please change decimal commas to points

Fig. 3 a Variation of bulk density (g/cm^3) of fired samples as function of temperature
Author please add these corrections to your Fig. 3 a:
Horizontal axis: Temperature / °C
Vertical axis: Bulk density / g/cm^3

Fig. 3 b Variation of bi-axial three points bending (MPa) of fired samples as function of temperature
Author please add these corrections to your Fig. 3 b:
Horizontal axis: Temperature / °C
Vertical axis: Bi-axial four points bending strength / MPa

Fig. 4 Variation of sintering parameters of three Kaolinitic clays with firing rate: 4 a (DSC) and 4 b (Dil)

Fig. 5 Formation of Ti-Al crystals in the matrixes of WAB (a) and MAY (b)

Fig. 6 Micrographs of the three Kaolinitic clays at 1500°C a) MAY at 1400 °C, b) WAB at 1400 °C, c) TAN 1400 °C

Fig. 7 Micrographs of fired Kaoilinitic clays at high temperauture showing the influence of glassy phase and impurities a) MAY 1500 °C, b) MAY 1500 °C, c) WAB 1500 °C, d) TAN 1500 °C

Bilder: Tabellen:

.

Table 1 Variation of structural parameters of mullite grains of fired kaolinitic clays as function of temperature / °C

	(Å)	1000	1100	1200	1300	1400	1500
	a	7.4694	7.3331	7.5564	7.5621	7.5533	7.5534
MAY	b	7.6863	7.4212	7.6969	7.6971	7.7071	7.7022
	c	2.7383	2.7131	2.8872	2.8878	2.8922	2.8927
	M*	18.09	24.34	70.35	74.35	76.67	79.07
	a	7.6299	7.5543	7.5548	7.5532	7.5544	7.5558
WAB	b	7.7387	7.7081	7.6977	7.7042	7.7059	7.7049
	c	2.8629	2.8875	2.8864	2.8863	2.8871	2.8913
	M*	19.94	33.59	60	67.99	70.32	73.61
	a			7.5626	7.5531	7.5515	7.5531
TAN	b			7.7051	7.7050	7.7044	7.7062
	c			2.8923	2.8864	2.8867	2.8867
	M*	0	0	9.68	29.28	34.30	40.47

M* is the proportion of mullite in mass-%

Figure 1:

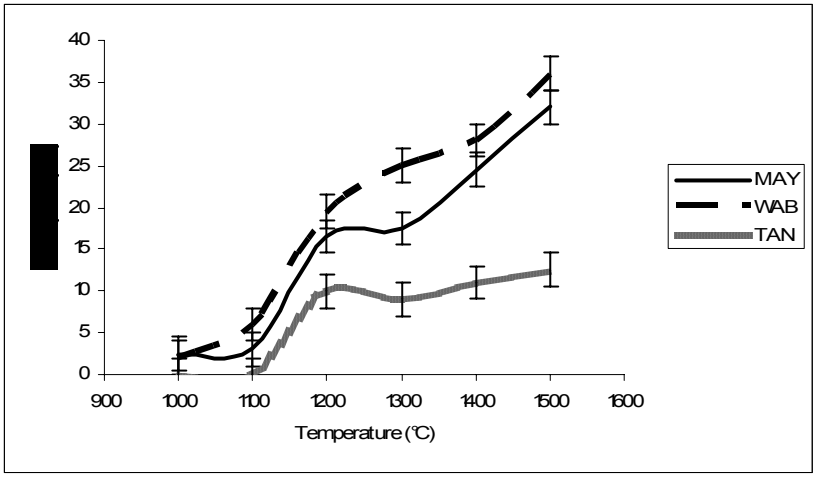

Figure 2:

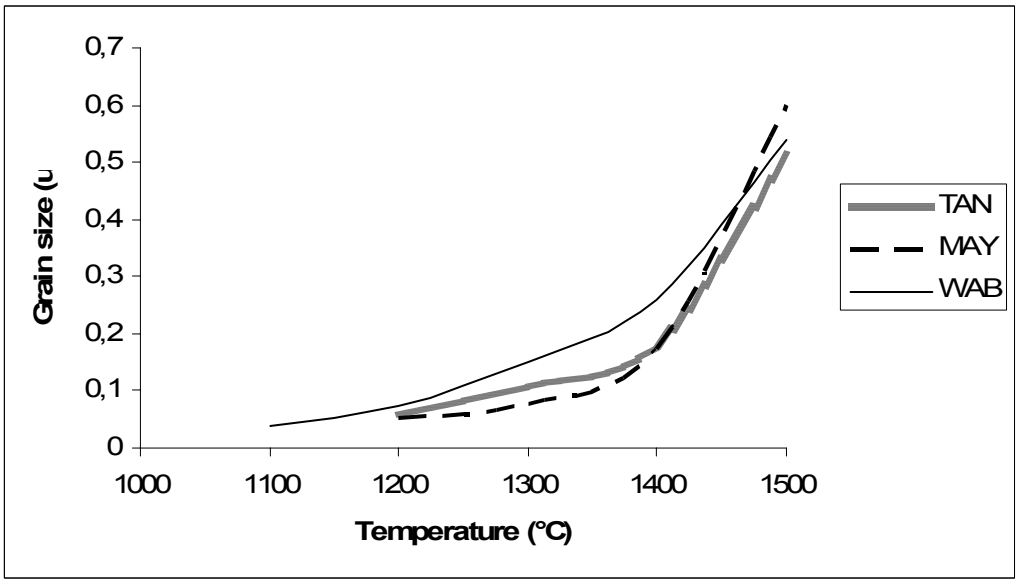

Figure 3a:

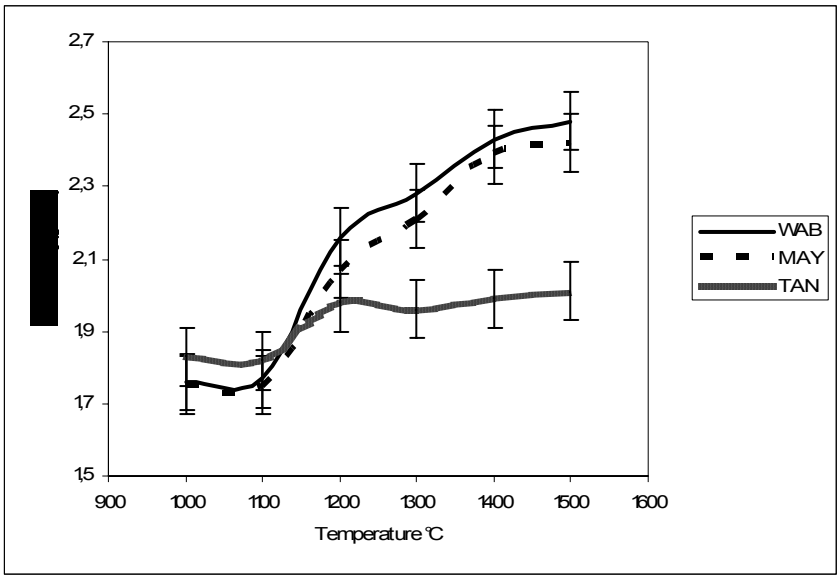

Figure 3b:

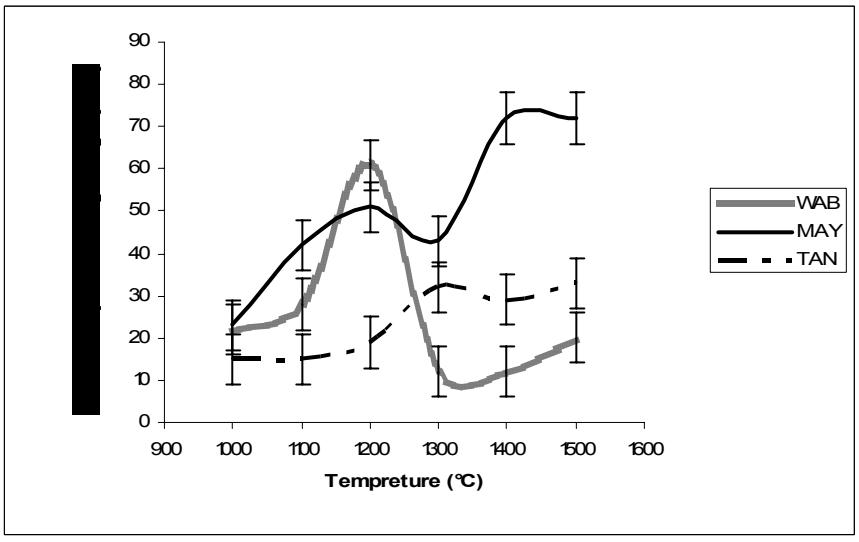

Figure 4a:

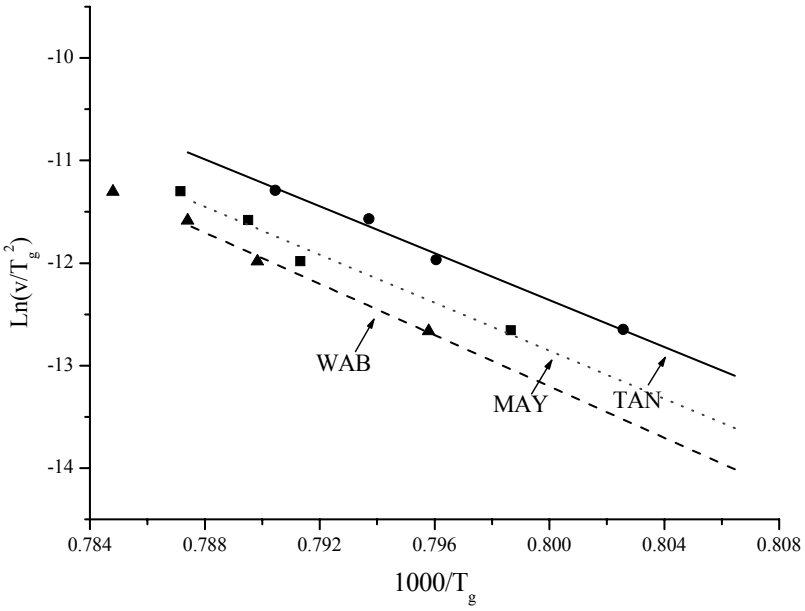

Figure 4b:

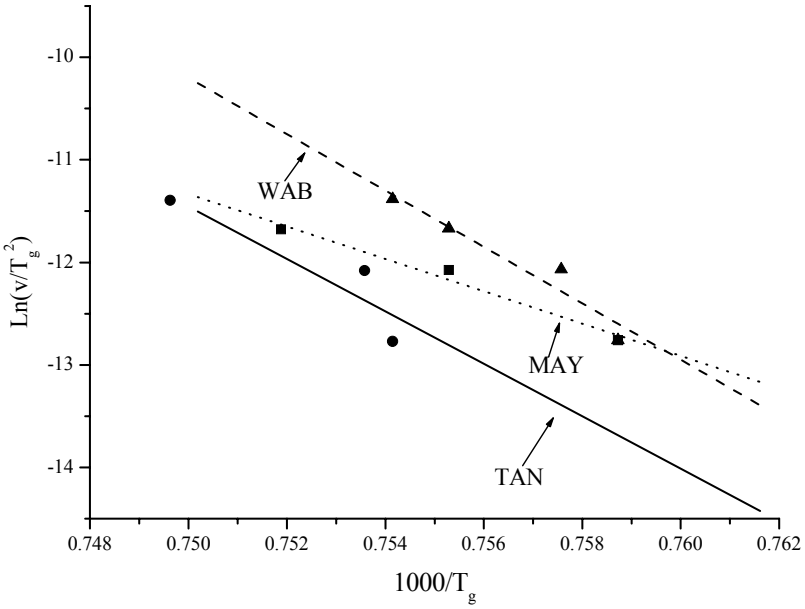

Figure 5

A **b**

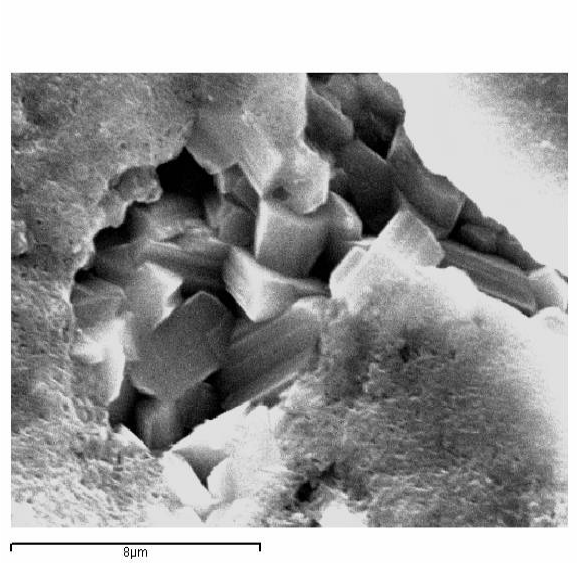

Figure 5

b

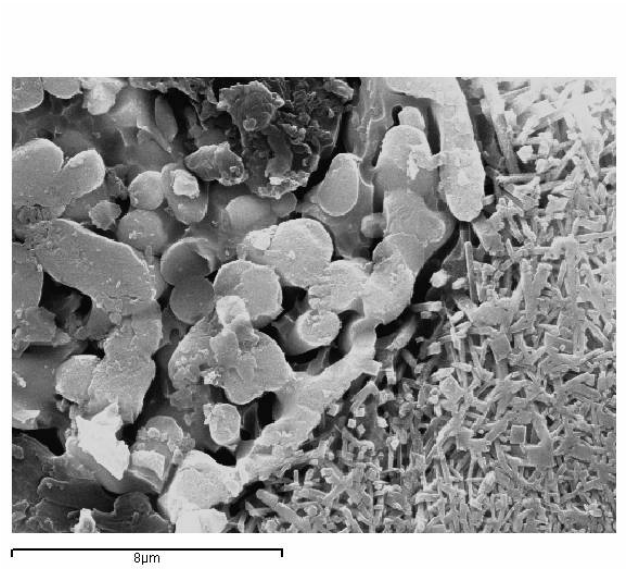

Figure 6: a) MAY at 1400°C

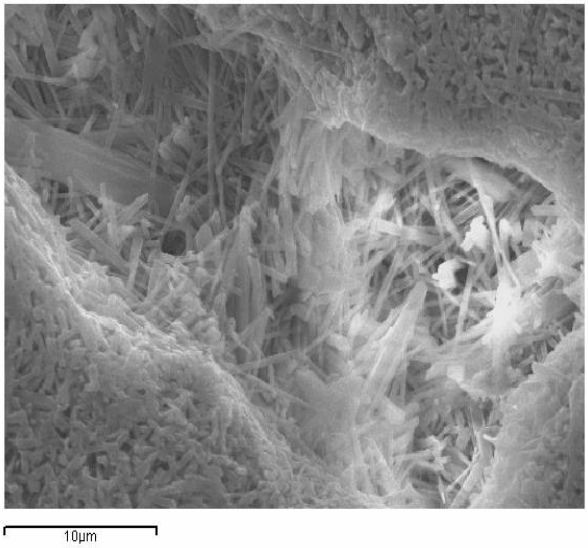

Figure 6 b) WAB at 1400°C

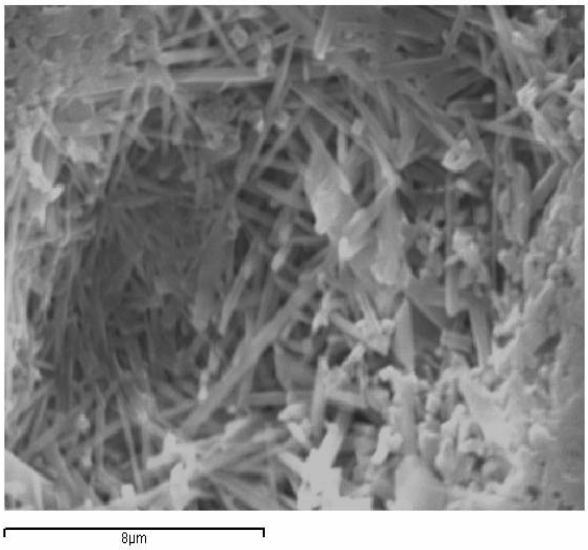

Figure 6 c) TAN 1400°C

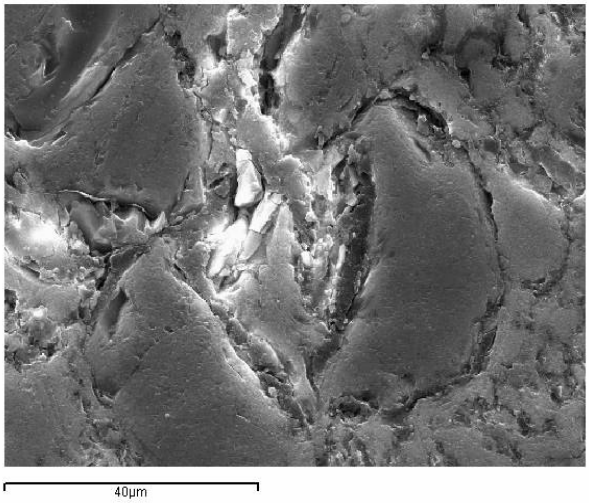

Figure 7:
a) MAY 1500°C

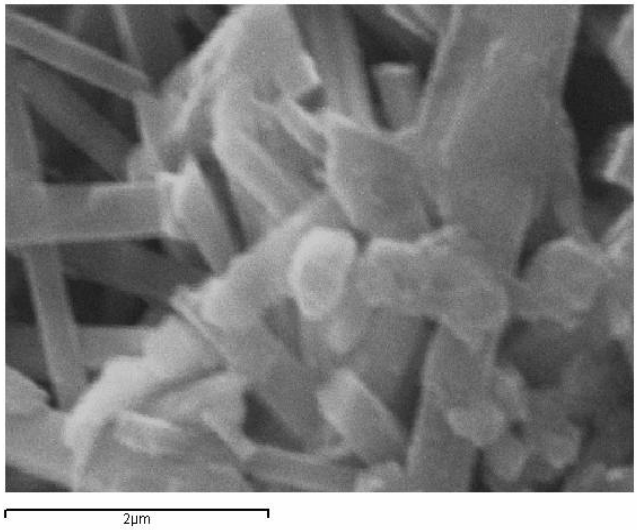

Figure 7:
b) AY 1500°C

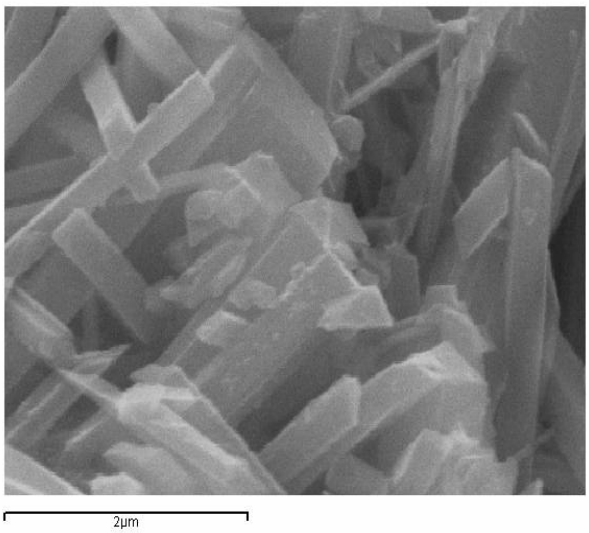

Figure 7:
c) WAB 1500°C

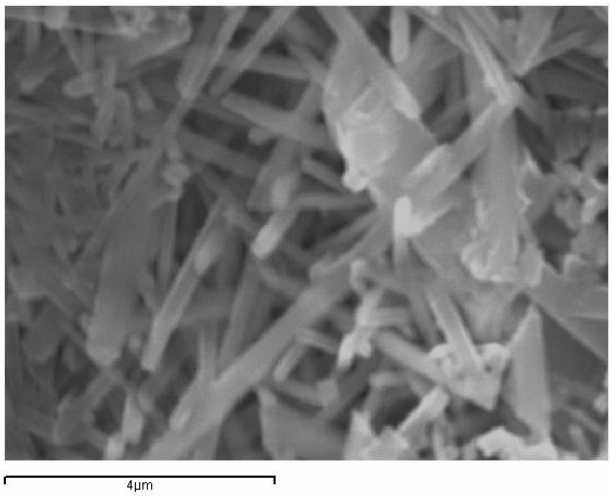

Figure 7:
d) TAN 1500°C

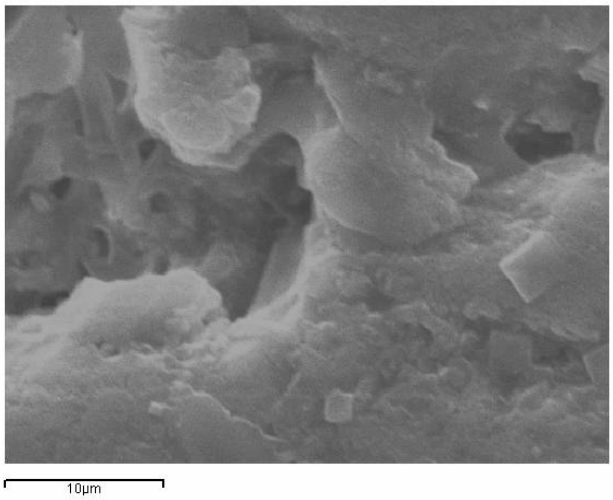
10µm